

Published in final edited form as:

J Am Chem Soc. 2012 August 8; 134(31): 13133–13140. doi:10.1021/ja3058502.

Synthesis and Self-Assembly Processes of Monofunctionalized Cucurbit[7]uril

 Brittany Vinciguerra[‡], Liping Cao[‡], Joe R. Cannon, Peter Y. Zavalij, Catherine Fenselau, and Lyle Isaacs^{*}

Department of Chemistry and Biochemistry, University of Maryland, College Park, MD 20742

Abstract

We present a building block approach toward functionalized CB[7] derivatives by the condensation of methylene bridged glycoluril hexamer **1** and glycoluril bis(cyclic ethers) **2** and **12**. The CB[7] derivatives Me₂CB[7] and CyCB[7] are highly soluble in water (264 mM and 181 mM, respectively). As a result of the high intrinsic solubility of Me₂CB[7], it is able to solubilize the insoluble benzimidazole drug albendazole. The reaction of hexamer **1** with glycoluril derivative **12** which bears a primary alkyl chloride group gives CB[7] derivative **18** in 16% isolated yield. Compound **18** reacts with NaN₃ to yield azide-substituted CB[7] **19** in 81% yield which subsequently undergoes click reaction with propargylammonium chloride (**21**) to yield CB[7] derivative **20** in 95% yield which bears a covalently attached triazolyl ammonium group along its equator. The results of NMR spectroscopy (¹H, variable temperature, and DOSY) and electrospray mass spectrometry establish that **20** undergoes self-assembly to form the cyclic tetrameric assembly (**20**₄) in aqueous solution. CB[7] derivatives bearing reactive functional groups (e.g. N₃, Cl) are now available for incorporation into more complex functional systems.

Introduction

The cucurbit[n]uril (CB[n]; n = 5, 6, 7, 8, 10) family of molecular containers^{1,2} is formed by the condensation reaction of glycoluril and formaldehyde under strongly acidic conditions.^{3,4,5} The defining structural features of the CB[n] compounds (Chart 1) are their two symmetry equivalent ureidyl C=O portals and their hydrophobic cavity which imparts the ability to bind to hydrophobic and cationic species in water by a combination of ion-dipole interactions and the hydrophobic effect.⁶ CB[n] compounds have emerged as a truly privileged class of receptors for molecular recognition in water as a result of their high affinity (K_a routinely 10⁶ – 10¹² M⁻¹), highly selective, and stimuli responsive binding processes.^{6–8} Accordingly, CB[n] compounds have been used in a wide range of applications including drug delivery,^{9,10,11} molecular machines,¹² supramolecular polymers,¹³ sensing ensembles,¹⁴ and biomimetic systems.¹⁵ Despite the wide range of applications that are enabled by CB[n] molecular containers there is an ongoing need for versatile synthetic approaches toward functionalized CB[n] compounds that retain their recognition properties and can be incorporated into more complex functional systems. Until quite recently, the only route to functionalized CB[n] compounds involved the direct (per)hydroxylation of CB[n] introduced by Kim.^{16,17} Kim and co-workers have used these

^{*}Corresponding Author: LIsaacs@umd.edu.

[‡]Author Contributions: These authors contributed equally.

 Supporting Information. Synthetic procedures, characterization data and ¹H and ¹³C NMR spectra for all new compounds, ¹H NMR spectra for host-guest complexes, details of the x-ray structure of Me₂CB[7]•**3**, ¹H NMR spectra used for K_{rel} calculation, ES-MS data for the decomposition reaction of Me₂CB[7], and MMFF minimized models of **20**₄. This material is available free of charge via Internet at <http://pubs.acs.org>.

functionalized CB[n] compounds in a variety of applications including nanocapsules for drug delivery, membrane protein fishing, and hydrogels for cellular engineering.^{10,18,19} Recently, Scherman and co-workers tamed the (per)hydroxylation reaction which allowed them to isolate (HO)₁CB[6] and perform subsequent functionalization reactions to deliver a self-complexing CB[6] derivative.²⁰

Our group has been investigating the mechanism of CB[n] formation^{21–24} as a route to prepare CB[n]-type receptors with exciting structures and functions. For example, we have used this mechanistic knowledge to prepare CB[n]-type receptors that display homotropic allostery, chiral recognition, and are useful in drug delivery applications.^{11,25} In 2011, we reported the templated synthesis of methylene bridged glycoluril hexamer **1** and its transformation into monofunctionalized CB[6] derivatives by macrocyclization reactions with substituted phthalaldehydes.²⁴ Very recently, we reported the synthesis of a clickable CB[6] derivative, its transformation into a CB[6] derivative functionalized with an ammonium ion tail, and its self-assembly into a cyclic [c2] daisy chain assembly.²⁶ Despite the recent advances in the synthesis of monofunctionalized CB[6] derivatives,^{20,24,26} there is still an unmet need for versatile synthetic routes toward CB[7] derivatives,^{16,18,27} and especially monofunctionalized CB[7] derivatives that are amenable to further functionalization reactions. For example, CB[7] is nicely soluble in water whereas CB[6] and the CB[6] derivatives prepared by us possess only modest solubility in the absence of guest. In addition, the more spacious cavity of CB[7] and its derivatives are able to bind to a wider variety of chemically and biologically interesting guests. Finally, the K_a values achieved with CB[7] are unsurpassed. In this paper we present a building block approach^{21,22,27,28,29,30} toward monofunctionalized CB[7] derivatives and report on their self-assembly behavior.

Results and Discussion

This results and discussion section is organized as follows. First, we discuss the preparation CB[7] derivatives Me₂CB[7], CyCB[7], and MePhCB[7] by a building block approach using glycoluril hexamer **1** and glycoluril bis(cyclic ethers) **2**. Then, we describe their basic properties (e.g. x-ray crystallography, host-guest binding, aqueous solubility, and drug solubilization). Next, we synthesize monofunctionalized CB[7] derivatives that contain reactive alkylchloride and azide functional groups. Finally, we describe the self-assembly of a CB[7] derivative to yield a cyclic tetrameric assembly in water.

Synthesis of Me₂CB[7] and CyCB[7]

Given the ready access to gram scale quantities of glycoluril hexamer **1** and glycoluril bis(cyclic ethers) **2** we decided to investigate their transformation into CB[7] derivatives (Scheme 1). After some experimentation, we performed the reaction between **1** and **2**_{Me} with added KI in 9 M H₂SO₄ at 110 °C for 30 minutes.³¹ Analysis of the crude reaction mixture using *p*-xylenediammonium ion (**3**) as ¹H NMR probe²⁴ showed the presence of a 55:45 ratio of CB[6] and Me₂CB[7]. As expected, the major competing reaction in this hexamer plus monomer building block approach to CB[7] derivatives is the unimolecular cyclization of hexamer to give CB[6]. Purification of the mixture was achieved by the addition of aqueous KI to an aqueous solution of the crude reaction mixture which results in precipitation of most of the CB[6] byproduct followed by final purification by treatment with activated carbon to yield Me₂CB[7] (380 mg) in 31% yield. A similar reaction was performed between **1** and **2**_{Cy} which delivered CyCB[7] in 18% yield. We find that Me₂CB[7] (264 mM) and CyCB[7] (181 mM) are significantly more soluble in water than CB[7] itself (20–30 mM)¹ which suggests that they might find utility in applications where highly soluble compounds are needed (e.g. supramolecular polymers or drug solubilization).³² When we performed related reactions with **2**_{Ph} or **2**_{CO₂Et} we did not

observe the formation of any CB[7] derivatives but rather observed the formation of CB[6] by unimolecular cyclization of **1**. From our previous work^{21,33} we know that **2_{Ph}** and **2_{CO₂Et}** are less reactive than alkylated glycolurils **2_{Me}** or **2_{Cy}** which makes them less able to undergo bimolecular reaction with **1** to give CB[7] derivatives. In contrast, however, a similar reaction between **1** and **2_{MePh}** resulted in a mixture of CB[6] and MePhCB[7] in a 61:30 ratio based on analysis of the crude ¹H NMR in the presence of **3**. Pure MePhCB[7] could only be obtained in a meager 3% yield after DowexTM ion exchange chromatography.

X-ray Crystal Structure of Me₂CB[7]

We were fortunate to obtain single crystals of Me₂CB[7] as its Me₂CB[7]•**3** complex and to solve its structure by X-ray crystallography. Figure 1a shows a cross eyed stereoview of the structure of the one of the Me₂CB[7]•**3** complexes in the crystal. In contrast to CB[6] derivatives which display an ellipsoidal deformation along their equator upon functionalization,^{24,29} the CB[7] derivative Me₂CB[7] appears structurally similar to CB[7] itself.⁴ For example, the distance between the ureidyl C=O O-atoms of a single glycoluril unit average 6.05 Å (range 5.87 – 6.154 Å) which is comparable to that observed for CB[7] (6.05 Å; range 5.913 – 6.114) itself. Similarly, the dimensions along the equator of Me₂CB[7] are comparable to that of CB[7] as well. For example, the distance between the opposing methine C-atoms on each fourth glycoluril on Me₂CB[7] averages 11.398 Å (range 11.247 – 11.516 Å) whereas CB[7] averages 11.404 Å (range 11.173 – 11.591 Å). One structural parameter that is rather different for CB[7] and Me₂CB[7] is the average distance between ureidyl C=O O-atoms on every fourth glycoluril at one portal. For Me₂CB[7] the distances average 8.188 Å (range 7.197 – 9.026 Å; standard deviation = 0.644 Å) whereas for CB[7] the distances average 8.139 Å (range 7.553 – 8.718 Å, standard deviation = 0.364 Å) for CB[7] itself. The glycolurils appear to pivot such that one O-atoms moves inward and one moves outward which results in the ureidyl C=O portals undergoing an ellipsoidal deformation. Overall, the molecular structures of the cavity of CB[7] and Me₂CB[7] are similar. Figure 1b shows a cross eyed stereoview of the basic packing of individual complexes of Me₂CB[7]•**3** into a square array parallel to the xy-plane within the crystal. The Me groups of two adjacent Me₂CB[7]•**3** complexes orient themselves toward each others ureidyl C=O portals. The iodide counterions (not depicted) are found at the corners of the square array and extend in columns along the z-axis.

Molecular Recognition Properties of Me₂CB[7] and CyCB[7]

After establishing the basic structural features of Me₂CB[7] we decided to investigate its molecular recognition properties. For this purpose, we used guests (**3** – **11**) shown in Chart 2 which increase in size from hexanediamine **4** to adamantane derivatives **9** – **11**. Guests **3** – **11** are well known to form complexes with unsubstituted CB[7] with binding constants up to $4.2 \times 10^{12} \text{ M}^{-1}$ for CB[7]•**9**.⁷ Figure 2 shows the ¹H NMR spectra recorded for Me₂CB[7]•**3**, Me₂CB[7]•**4**, Me₂CB[7]•**7**, and Me₂CB[7]•**10**. The guest resonances observed in ¹H NMR spectra are nearly identical in chemical shift to those measured for the corresponding CB[7] complexes (Supporting Information) which indicates that the magnetic environment inside the cavity of CB[7] and Me₂CB[7] are quite similar. The resonances observed in the ¹H NMR spectra that correspond to the H-atoms of C_{2v}-symmetric Me₂CB[7] reflect its lower symmetry. For example, three doublets of relative integral two and one doublet of relative integral one are observed for the upfield shifted H-atoms of the diastereotopic CH₂-groups of the Me₂CB[7]•**3** complex (Figure 2a). The main reason for synthesizing CB[7] derivatives is to be able to incorporate them into more complex systems while maintaining their recognition properties. Therefore, we viewed it as critical to verify that the high binding constants observed for CB[7] are maintained for CB[7] derivatives like Me₂CB[7]. For this purpose, we used the complexes CB[7]•**11** and Me₂CB[7]•**11** because the H-atoms adjacent to the pyridinium N-atom are located at the ureidyl C=O portal in the

complexes. Given that the presence of the two Me groups induce a change in the O•••O distance in the substituted glycoluril (*vide supra*) we thought that these protons might exhibit different chemical shifts in the CB[7]•**11** and Me₂CB[7]•**11** complexes.

Experimentally, we find that H_n resonates at 8.95 ppm for CB[7]•**11** and 8.96 ppm for Me₂CB[7]•**11** (Supporting Information). We used a ¹H NMR competition experiment (Supporting Information) to determine that the K_a value for Me₂CB[7]•**11** is 3.2 × 10¹² M⁻¹ relative to the known K_a value for CB[7]•**11** (1.98 × 10¹² M⁻¹).⁷ Accordingly, it seems reasonable to expect that CB[7] derivatives like Me₂CB[7] will function well as CB[7] surrogates in more complicated systems.

Stability of Me₂CB[7]

Experiments performed by Day and coworkers established that CB[5], CB[6], and CB[7] are quite stable under the hot acidic conditions (conc. HCl, 100 °C, 24 h) used in their formation.⁵ Accordingly, we wondered whether the Me substituents on the convex face of Me₂CB[7] might stabilize cationic intermediates accessible under acidic conditions and thereby accelerate decomposition reactions of Me₂CB[7]. Figure 3 shows a plot of the mole fraction of Me₂CB[7] versus time for a solution of Me₂CB[7] heated at 110 °C in 9M H₂SO₄. Over the course of 6 days, Me₂CB[7] completely decomposes. The ¹H NMR spectrum of the crude reaction mixture using **3** as probe after 6 days shows the presence of macrocycles with CB[6] sized cavities (≈ 24% of the crude mixture). Electrospray mass spectrometry of the crude reaction mixture allows us to identify the presence of comparable amounts of CB[6] and Me₂CB[6]. Given that few applications require such highly acidic and high temperature conditions, we believe that dialkylated CB[7] derivatives will be sufficiently stable in most situations.

Drug Solubilization Using Me₂CB[7]

One of the emerging application areas of CB[n] molecular containers involves their use as solubilizing excipients for insoluble pharmaceutical agents.^{11,34} Given the high solubility of Me₂CB[7] in water we decided to test its ability to solubilize albendazole and camptothecin which have previously been solubilized by unsubstituted CB[7].³⁵ Figure 4 shows the phase solubility diagrams constructed for albendazole with either Me₂CB[7] or CB[7]. To construct the phase solubility diagrams³⁶ we stirred a solution of a known concentration of host with an excess of insoluble drug overnight, filtered the solution to remove excess insoluble drug, and measured the concentration of soluble drug by ¹H NMR using CH₃SO₃⁻ as a non-binding internal standard of known concentration. The phase solubility diagrams for albendazole and Me₂CB[7] or CB[7] are quite similar at low concentrations of container (up to 10 mM). This result can be explained by the fact that the linear region of phase solubility diagrams for 1:1 host:guest complexes obey equation 1 where K_a is the host•guest binding constant (M⁻¹) and s₀ is the intrinsic solubility of guest (drug). Given that s₀ for albendazole is the same regardless of which host is used and that the K_a values for the CB[7]•albendazole and Me₂CB[7]•albendazole are expected to be very similar, then the initial slopes should also be very similar according to equation 1. Somewhat surprisingly, at higher concentrations of Me₂CB[7] (e.g. 25 – 50 mM), the concentration of albendazole in solution reaches a plateau of 5.8 mM which is lower than that achieved with 15 mM CB[7] (8.1 mM). The plateau in the phase solubility diagram for Me₂CB[7]•albendazole indicates that the complex possesses only moderate solubility in water (≈ 5.8 mM). Why does Me₂CB[7] – which is far more water soluble CB[7] – perform less well in the solubilization of albendazole? We believe that the introduction of the Me groups on the convex face of uncomplexed Me₂CB[7] dramatically increases its solubility relative to CB[7] because they prevent the CH•••O interactions between the methine C-H groups on the convex face of one container with the ureidyl C=O portals of another container in the solid state which has been implicated as a controlling factor in the solubility trends of CB[n] compounds.³⁷ Within the

Me₂CB[7]•albendazole and CB[7]•albendazole complexes the drug fills the cavity and protrudes through the ureidyl C=O portals. Accordingly, the Me groups cannot enhance the solubility of Me₂CB[7]•albendazole in the same way as they do Me₂CB[7]. On the contrary, the presence of the hydrophobic Me groups decrease the solubility of Me₂CB[7]•albendazole relative to CB[7]•albendazole. A similar trend was noted for the solubilization of camptothecin by CB[7] and Me₂CB[7] (Supporting Information). These result suggest that a major consideration in the design of CB[n] derivatives for use as solubilizing excipients is the incorporation of groups designed to enhance the solubility of both the container and its container•drug complexes.

$$K_a = \frac{\text{slope}}{s_0(1-\text{slope})} \quad (1)$$

Synthesis of glycoluril derivative **12**

The preparation of glycoluril derivative **12**³⁰ bearing a primary alkyl chloride is shown in Scheme 3. First, we react butanedione **13** with isopropylamine **14** in Et₂O with TiCl₄ to deliver the known diimine **15**.³⁸ Next, we deprotonated **15** with LDA in THF followed by subsequent alkylation with 3-iodo-1-chloropropane to yield **16** in 69% yield after hydrolytic workup.³⁹ Compound **16** was transformed into glycoluril **17** by reaction with urea in HCl at room temperature in 35% yield. Finally, treatment of **17** with formalin in HCl gives **12** in 68% yield.

Synthesis of Monofunctionalized CB[7] Derivatives **18 – 20**

With access to gram scale quantities of **12** we decided to synthesize monofunctionalized CB[7] derivative **18** (Scheme 3). The reaction between **1** and **12** was conducted in 9M H₂SO₄ at 110 °C in the presence of KI as developed for the synthesis of Me₂CB[7], CyCB[7], and MePhCB[7] described above. The ¹H NMR spectrum of the crude reaction mixture obtained using **3** as probe allowed us to estimate that **18** comprised 66% of the crude material. Purification by Dowex™ ion exchange chromatography allowed us to isolate 210 mg **18** in pure form in 16% yield. Clearly, the purification process is far from ideal and we are working to improve the process. We found that **18** can be transformed into monofunctionalized CB[7] derivative **19** which contains a reactive azide functional group in 81% yield by simply heating with NaN₃ in H₂O at 80 °C for 2 days. Azide **19** reacts with propargyl ammonium chloride (**21**) in the presence of Pericàs' catalyst⁴⁰ in H₂O at 50 °C to give **20** in 95% yield. The ¹H NMR spectrum of the purified sample of **20** in the presence of **3** – which is a strong binder for CB[7] sized cavities⁷ and thereby disrupts any potential self-assembly processes of **20** – is shown in Figure 5a.

Self-Assembly of **20** to Yield Cyclic Tetramer **20₄**

We anticipated that **20** which contains both a CB[7] sized cavity and a covalently attached triazolyl ammonium ion – which is a good guest for CB[7] sized cavities – would undergo self assembly processes in water. A priori it was hard to predict whether supramolecular polymerization processes or formation of discrete cyclic assemblies would predominate.⁴¹ Figure 5b shows the ¹H NMR spectrum recorded for a 3.3 mM solution of **20** in D₂O at room temperature. A single relatively sharp triazole C-H resonance is observed at 6.45 ppm which suggested the formation of a well defined assembly. On the other hand, the upfield region of the spectrum between 2.70 and 1.00 ppm corresponding to the (CH₂)₄ linker between the CB[7] moiety and the triazole binding unit are broadened and the presence of several groups of resonances suggested the presence of several different assemblies. Figure 5c shows the ¹H NMR spectrum recorded at 80 °C which shows that these different groups

of resonances coalesce and sharpen into four distinct resonances corresponding to each of the four CH₂-groups of the linking chain. The fact that the resonances for H_t and H_u are still strongly upfield shifted in the ¹H NMR spectrum recorded at 80°C (Figure 5b versus 5c) suggests that the assembly **20_n** persists at high temperature. To gain insight into the degree of oligomerization (n) of the self-assembled species (**20_n**) formed in D₂O we performed diffusion ordered spectroscopy (DOSY)⁴² for the monomeric complex **20•3** and for the self-assembled species **20_n** as shown in Figure 6. The diffusion coefficients measured using four different resonances for **20•3** and **20_n** averaged $2.646 \pm 0.026 \times 10^{-10} \text{ m}^2 \text{ s}^{-1}$ and $1.638 \pm 0.045 \times 10^{-10} \text{ m}^2 \text{ s}^{-1}$, respectively (Figure 6). The ratio of diffusion constants for **20•3** and **20_n** is 1.616. The Stokes-Einstein equation (eq. 2) shows the relationship between the diffusion coefficient (D) and the hydrodynamic radius (r_s) in a medium of viscosity η where k_B is Boltzmann's constant and T is temperature.⁴² If we assume that **20•3** and **20_n** are roughly spherical then the ratio of the measured diffusion coefficients can be converted into a ratio of molecular weights which gives the oligomerization number. For a trimeric, tetrameric, or pentameric assembly theory predicts the ratio D(**20•3**)/D(**20_n**) = 1.442 (n = 3), 1.587 (n = 4), and 1.709 (n = 5). In this manner, the measured ratio of diffusion coefficients of 1.616 strongly suggests the formation of the cyclic tetrameric assembly **20₄**.

$$D = k_B T / 6\pi\eta r_s \quad (2)$$

To provide additional evidence for the formation of the cyclic tetrameric assembly **20₄** we performed electrospray ionization mass spectrometry of 100 μM solutions in H₂O and 100,000 resolution on an LTQ-Orbitrap instrument (ThermoFisher, San Jose, CA). Figure 7a shows the mass spectrum obtained which shows a 4+ ion at *m/z* = 1329.97, a 5+ ion at *m/z* = 1068.68, and a 6+ at *m/z* = 894.31. The 4+ ion corresponds to the **20₄⁴⁺** assembly. Figure 7b shows the expansion of the region of the **20₄⁴⁺** ion and Figure 7c shows the theoretical ion distribution for molecular formula C₂₀₀H₂₂₈N₁₂₈O₅₆. The excellent match between Figure 7b and 7c provides strong evidence for the description of this structure as the cyclic tetramer **20₄⁴⁺**. Other ions of significant intensity in Figure 7a were observed at *m/z* = 1068.68 which corresponds to [**20₄•Na**]⁵⁺ and *m/z* = 894.31 which corresponds to [**20₄•Na₂**]⁶⁺. To gain further insight into this system, we isolated ion **20₄⁴⁺** and performed collisional induced dissociation experiments (Figure 7d). We observed the cleavage of covalent bonds rather than the expected dissociation of non-covalent aggregate **20₄⁴⁺** into smaller non-covalent aggregate ions (e.g. monomers, dimers, or trimers). Overall, the electrospray mass spectrometric investigations strongly support that **20** self-assembles to give a highly stable cyclic tetrameric aggregate **20₄⁴⁺**.

Enumeration of the Different Diastereomers of **20₄**

Although compound **1** is achiral due to the presence of a mirror plane that runs through the equator of the molecule, complexation events that desymmetrize the cavity result in the formation of complexes that are enantiomers and the two C=O portals can be described as enantiotopic. Accordingly, when four molecules of **1** self-assemble to form **1₄**, there are several diastereomers that can form (Scheme 4). For example, all four Me groups can be pointing up (u,u,u,u-**1₄**), three up and one down (u,u,u,d-**1₄**), and two different combinations of two up and two down (u,u,d,d-**1₄** and u,d,u,d-**1₄**).⁴³ The various diastereomers are able to interconvert with one another by a sequence of dissociation of one of the CB[7]•triazolyl ammonium complexes to give a linear tetramer, followed by rotation of the CB[7] group and recomplexation of the triazolyl ammonium through the opposite ureidyl C=O portal of the CB[7] moiety. In this way, the averaging of the signals observed in the high temperature ¹H NMR spectrum shown in Figure 5c is readily understandable.

Conclusion

In summary, we have shown that CB[7] derivatives are accessible by a building block approach that involves the condensation of glycoluril hexamer **1** with glycoluril bis(cyclic ethers) **2**_{Me}, **2**_{Cy}, **2**_{MePh}, and **12**. Just like CB[7] itself, the high water solubility of Me₂CB[7] and its outstanding host-guest recognition properties make it well suited as a solubilization agent for poorly soluble pharmaceutical agents. Compound **18** which bears a reactive primary alkylchloride group is the first monofunctionalized CB[7] derivative to be reported. Compound **18** undergoes further functionalization reactions to yield **19** and subsequently **20** by click chemistry. We find that **20** undergoes a self-assembly process in water to yield cyclic tetramer **1**₄ as established by NMR (VT and DOSY) and mass spectrometric measurements.

We believe that the implications of this research go well beyond the system specific details described above. For example, unfunctionalized CB[7] has been the most widely applied CB[n] compound because of its good solubility in water and its exceptional binding affinity and selectivity toward its guests in water. This paper provides two water soluble monofunctionalized CB[7] derivatives that are amenable to further functionalization reactions by S_N2 and click chemistry which promises to allow the homogenous covalent attachment of CB[7] to solid phases, macromolecules like proteins and polymers, and incorporation into other complex and functional (bio)molecular systems. When that occurs, the continued impact of the CB[n] family of molecular containers on the chemical sciences will be significant.

Experimental

Compound 18

A mixture of **1** (1.00 g, 1.03 mmol) and KI (0.230 g, 1.35 mmol) were dissolved in 9M aqueous H₂SO₄ (5 mL) and then treated with **12** (0.510 g, 1.55 mmol). The flask was then sealed with a rubber septum and heated at 110 °C for 30 min. The reaction solution was poured into MeOH (40 mL) which resulted in a gray precipitate. The mixture was centrifuged at 7200 rpm for 5 min. The supernatant was decanted and the precipitate was washed with MeOH (40 mL × 3) and centrifuged at 7200 rpm for 5 min. The precipitate was dried under high vacuum to give a crude, gray powder (1.46 g). The crude solid was dissolved in 88% formic acid/0.4 M HCl (1:1, v:v, 10 mL). The solution containing the crude solid was loaded onto a column (3 cm diameter × 20 cm long) containing Dowex 50WX2 ion-exchange resin pretreated with 88% formic acid/0.4 M HCl (1:1, v:v). The column was eluted with 88% formic acid/0.4 M HCl (1:1, v:v, 400 mL), and then 88% formic acid/0.6 M HCl (1:1, v:v, 400 mL), and then 88% formic acid/0.8 M HCl (1:1, v:v, 400 mL). The fraction purity was assessed by ¹H NMR using **3** as a probe. The appropriate fractions were combined and solvent was removed by rotary evaporation and dried under high vacuum. The yellow solid was then washed with MeOH (40 mL) and centrifuged at 7200 rpm for 5 min. The supernatant was decanted and the precipitate was dried under high vacuum to give **18** as a white powder (0.21 g, 0.16 mmol, 16%). M.p. > 300 °C. IR (KBr, cm⁻¹): 3001w, 2917w, 1729s, 1479s, 1423m, 1376m, 1321s, 1290m, 1235s, 1193s, 968m, 828m, 807s. ¹H NMR (500 MHz, D₂O, >1 equiv. **3**): 7.51 (s, unbound **3**), 6.62 (s, 4H), 5.80-5.65 (m, 14H), 5.60-5.40 (m, 12H), 4.40-4.20 (m, 10H), 4.21 (s, unbound **3**), 4.16 (d, *J* = 15.4, 4H), 3.92 (s, 4H), 3.64 (t, *J* = 6.3, 2H), 2.40-2.30 (m, 2H), 1.90 (s, 3H), 1.95-1.85 (m, 2H), 1.40-1.30 (m, 2H). ¹³C NMR (125 MHz, D₂O, dioxane as internal reference, >1 equiv. **3**): 156.8, 156.7, 156.5, 156.5, 156.5, 156.2, 133.7, 133.6, 129.6, 128.0, 80.5, 78.8, 71.7, 71.6, 71.5, 71.4, 71.3, 71.2, 71.2, 71.1, 70.3, 53.2, 53.1, 52.6, 52.6, 52.3, 49.3, 48.9, 44.8, 42.7, 42.4, 31.2, 27.4, 19.6, 14.7 (only 35 of the 39 resonances expected were observed). HR-MS: *m/z* 702.2476 ([**18**•**3**]²⁺, calcd. for C₄₇H₅₁ClN₂₈O₁₄•C₈H₁₄N₂²⁺, 702.2493).

Compound 19

A mixture of **18** (100 mg, 0.079 mmol) and NaN_3 (39 mg, 0.60 mmol) were dissolved in H_2O (2 mL). The mixture was heated at 80 °C for 2 days. The reaction solution was poured into MeOH (3 mL) which resulted in a gray precipitate. The mixture was centrifuged at 7200 rpm for 5 min. The supernatant was decanted and the precipitate was washed with MeOH (5 mL \times 3) and centrifuged at 7200 rpm for 5 min. The precipitate was dried under high vacuum to give **19** as a white powder (81 mg, 0.064 mmol, 81%). M.p. > 300 °C. IR (KBr, cm^{-1}): 3442m, 3001w, 2923w, 2099w, 2034m, 1729s, 1476s, 1420m, 1378m, 1322m, 1236s, 1192m, 971m. ^1H NMR (400 MHz, D_2O , >1 equiv. **3**): 7.47 (s, unbound **3**), 6.62 (s, 4H), 5.80-5.60 (m, 14H), 5.60-5.40 (m, 12H), 4.35 (d, $J = 16.0$, 2H), 4.29 (d, $J = 15.6$, 4H), 4.23 (d, $J = 15.6$, 2H), 4.22 (d, $J = 15.6$, 2H), 4.15 (d, $J = 15.6$, 4H), 4.13 (s, unbound **3**), 3.91 (s, 4H), 3.36 (t, $J = 6.2$, 2H), 2.40-2.30 (m, 2H), 1.89 (s, 3H), 1.75-1.65 (m, 2H), 1.35-1.25 (m, 2H). ^{13}C NMR (125 MHz, D_2O , dioxane as internal reference, >1 equiv. **3**): 156.7, 156.6, 156.5, 156.5, 156.4, 156.2, 134.3, 134.3, 128.3, 127.8, 80.4, 78.8, 71.7, 71.6, 71.6, 71.5, 71.4, 71.3, 71.2, 71.2, 71.0, 70.3, 53.1, 53.0, 52.6, 52.5, 52.3, 50.6, 49.2, 48.8, 43.9, 42.6, 27.6, 19.6, 14.7 (only 35 of the 39 resonances expected were observed). HR-MS: m/z 705.7703 ($[\mathbf{19}\cdot\mathbf{3}]^{2+}$, calcd. for $\text{C}_{47}\text{H}_{51}\text{N}_{31}\text{O}_{14}\cdot\text{C}_8\text{H}_{14}\text{N}_2^{2+}$, 705.7694).

Compound 20

A mixture of **19** (50 mg, 0.039 mmol) and propargyl amine hydrochloride (**21**, 36 mg, 0.39 mmol), and Pericàs' catalyst (0.0039 mmol, 2.4 mg)⁴⁰ were dissolved in H_2O (2 mL). The mixture was heated at 50 °C for 1 day. The reaction solution was poured into MeOH (3 mL) which resulted in a gray precipitate. The mixture was centrifuged at 7200 rpm for 5 min. The supernatant was decanted and the precipitate was washed with MeOH (5 mL \times 3) and centrifuged at 7200 rpm for 5 min. The precipitate was dried under high vacuum to give **20** as a white powder (50 mg, 0.037 mmol, 95%). M.p. > 300 °C. IR (KBr, cm^{-1}): 3442m, 2994w, 2916w, 1729s, 1473s, 1422m, 1378m, 1322m, 1235s, 1194m, 970m. ^1H NMR (500 MHz, D_2O , >1 equiv. **3**): 8.10 (s, 1H), 7.50 (s, unbound **3**), 6.61 (s, 4H), 5.80-5.60 (m, 14H), 5.60-5.40 (m, 12H), 4.48 (t, $J = 6.3$, 2H), 4.32 (s, 2H), 4.35-4.20 (m, 10H), 4.20 (s, unbound **3**), 4.15 (d, $J = 15.4$, 4H), 3.89 (s, 4H), 2.40-2.30 (m, 2H), 2.10-2.00 (m, 2H), 1.79 (s, 3H), 1.15-1.05 (m, 2H). ^{13}C NMR (125 MHz, D_2O , dioxane as internal reference, >1 equiv. **3**): 156.7, 156.7, 156.5, 156.5, 156.5, 156.1, 133.7, 133.6, 129.6, 128.0, 125.4, 80.4, 78.7, 71.7, 71.6, 71.5, 71.4, 71.3, 71.2, 71.2, 71.1, 53.2, 53.1, 52.6, 52.6, 52.3, 49.9, 49.2, 48.8, 42.7, 42.4, 34.0, 28.8, 27.4, 19.1, 14.7 (only 36 of the 42 resonances expected were observed). HR-MS: m/z 733.2910 ($[\mathbf{20}\cdot\mathbf{3}]^{2+}$, calcd. for $\text{C}_{50}\text{H}_{56}\text{N}_{32}\text{O}_{14}\cdot\text{C}_8\text{H}_{14}\text{N}_2^{2+}$, 733.2905).

Supplementary Material

Refer to Web version on PubMed Central for supplementary material.

Acknowledgments

We thank Dr. Derick Lucas for initial experiments directed toward the preparation of $\text{Me}_2\text{CB}[7]$. We thank the National Science Foundation (CHE-1110911 to L.I.) and the National Institutes of Health (GM021248 to C.F.) for financial support. This paper is dedicated to Professor François Diederich – inspiring mentor and outstanding scientist – on the occasion of his 60th birthday.

References

1. Lee JW, Samal S, Selvapalam N, Kim HJ, Kim K. Acc Chem Res. 2003; 36:621–630. [PubMed: 12924959]

2. Lagona J, Mukhopadhyay P, Chakrabarti S, Isaacs L. *Angew Chem, Int Ed.* 2005; 44:4844–4870. Nau WM, Florea M, Assaf KI. *Isr J Chem.* 2011; 51:559–577. Masson E, Ling X, Joseph R, Kyeremeh-Mensah L, Lu X. *RSC Adv.* 2012; 2:1213–1247.
3. Freeman WA, Mock WL, Shih NY. *J Am Chem Soc.* 1981; 103:7367–7368. Day AI, Blanch RJ, Arnold AP, Lorenzo S, Lewis GR, Dance I. *Angew Chem, Int Ed.* 2002; 41:275–277. Liu S, Zavalij PY, Isaacs L. *J Am Chem Soc.* 2005; 127:16798–16799. [PubMed: 16316221]
4. Kim J, Jung IS, Kim SY, Lee E, Kang JK, Sakamoto S, Yamaguchi K, Kim K. *J Am Chem Soc.* 2000; 122:540–541.
5. Day AI, Arnold AP, Blanch RJ, Snushall B. *J Org Chem.* 2001; 66:8094–8100. [PubMed: 11722210]
6. Mock WL, Shih NY. *J Org Chem.* 1986; 51:4440–4446.
7. Liu S, Ruspic C, Mukhopadhyay P, Chakrabarti S, Zavalij PY, Isaacs L. *J Am Chem Soc.* 2005; 127:15959–15967. [PubMed: 16277540]
8. Rekharsky MV, Mori T, Yang C, Ko YH, Selvapalam N, Kim H, Sobransingh D, Kaifer AE, Liu S, Isaacs L, Chen W, Moghaddam S, Gilson MK, Kim K, Inoue Y. *Proc Natl Acad Sci U S A.* 2007; 104:20737–20742. [PubMed: 18093926]
9. Uzunova VD, Cullinane C, Brix K, Nau WM, Day AI. *Org Biomol Chem.* 2010; 8:2037–2042. [PubMed: 20401379] McInnes FJ, Anthony NG, Kennedy AR, Wheate NJ. *Org Biomol Chem.* 2010; 8:765–773. [PubMed: 20135032] Angelos S, Khashab NM, Yang YW, Trabolsi A, Khatib HA, Stoddart JF, Zink JI. *J Am Chem Soc.* 2009; 131:12912–12914. [PubMed: 19705840] Zhang J, Coulston RJ, Jones ST, Geng J, Scherman OA, Abell C. *Science.* 2012; 335:690–694. [PubMed: 22323815]
10. Kim E, Kim D, Jung H, Lee J, Paul S, Selvapalam N, Yang Y, Lim N, Park CG, Kim K. *Angew Chem, Int Ed.* 2010; 49:4405–4408.
11. Ma D, Hettiarachchi G, Nguyen D, Zhang B, Wittenberg JB, Zavalij PY, Briken V, Isaacs L. *Nat Chem.* 2012; 4:503–510. [PubMed: 22614387]
12. Jeon WS, Ziganshina AY, Lee JW, Ko YH, Kang JK, Lee C, Kim K. *Angew Chem, Int Ed.* 2003; 42:4097–4100. Ko YH, Kim E, Hwang I, Kim K. *Chem Commun.* 2007:1305–1315. Jeon WS, Kim E, Ko YH, Hwang I, Lee JW, Kim SY, Kim HJ, Kim K. *Angew Chem, Int Ed.* 2005; 44:87–91.
13. Appel EA, Biedermann F, Rauwald U, Jones ST, Zayed JM, Scherman OA. *J Am Chem Soc.* 2010; 132:14251–14260. [PubMed: 20845973] Wang W, Kaifer AE. *Angew Chem, Int Ed.* 2006; 45:7042–7046. Kim K, Kim D, Lee JW, Ko YH, Kim K. *Chem Commun.* 2004:848–849. Liu Y, Yu Y, Gao J, Wang Z. *Angew Chem, Int Ed.* 2010; 49:6576–6579.
14. Ghale G, Ramalingam V, Urbach AR, Nau WM. *J Am Chem Soc.* 2011; 133:7528–7535. [PubMed: 21513303] Biedermann F, Rauwald U, Cziferszky M, Williams KA, Gann LD, Guo BY, Urbach AR, Bielawski CW, Scherman OA. *Chem Eur J.* 2010; 16:13716–13722. [PubMed: 21058380] Baumes LA, Sogo MB, Montes-Navajas P, Corma A, Garcia H. *Chem Eur J.* 2010; 16:4489–4495. [PubMed: 20309968] Wu J, Isaacs L. *Chem Eur J.* 2009; 15:11675–11680. [PubMed: 19774569]
15. Liu S, Zavalij PY, Lam YF, Isaacs L. *J Am Chem Soc.* 2007; 129:11232–11241. [PubMed: 17696539] Ghosh S, Isaacs L. *J Am Chem Soc.* 2010; 132:4445–4454. [PubMed: 20210325] Kim C, Agasti SS, Zhu Z, Isaacs L, Rotello VM. *Nat Chem.* 2010; 2:962–966. [PubMed: 20966953] Nguyen HD, Dang DT, van Dongen JLJ, Brunsveld L. *Angew Chem, Int Ed.* 2010; 49:895–898. Chinai JM, Taylor AB, Ryno LM, Hargreaves ND, Morris CA, Hart PJ, Urbach AR. *J Am Chem Soc.* 2011; 133:8810–8813. [PubMed: 21473587]
16. Jon SY, Selvapalam N, Oh DH, Kang JK, Kim SY, Jeon YJ, Lee JW, Kim K. *J Am Chem Soc.* 2003; 125:10186–10187. [PubMed: 12926937]
17. Kim K, Selvapalam N, Ko YH, Park KM, Kim D, Kim J. *Chem Soc Rev.* 2007; 36:267–279. [PubMed: 17264929]
18. Lee DW, Park KM, Banerjee M, Ha SH, Lee T, Suh K, Paul S, Jung H, Kim J, Selvapalam N, Ryu SH, Kim K. *Nat Chem.* 2011; 3:154–159. [PubMed: 21258389]
19. Park KM, Yang J-A, Jung H, Yeom J, Park JS, Park K-H, Hoffman AS, KHS, Kim K. *ACS Nano.* 2012; 6:2960–2968. [PubMed: 22404424]
20. Zhao N, Lloyd GO, Scherman OA. *Chem Commun.* 2012; 48:3070–3072.

21. Chakraborty A, Wu A, Witt D, Lagona J, Fettinger JC, Isaacs L. *J Am Chem Soc.* 2002; 124:8297–8306. [PubMed: 12105910]
22. Huang WH, Zavalij PY, Isaacs L. *J Am Chem Soc.* 2008; 130:8446–8454. [PubMed: 18529059]
23. Ma D, Gargulakova Z, Zavalij PY, Sindelar V, Isaacs L. *J Org Chem.* 2010; 75:2934–2941. [PubMed: 20345157]
24. Lucas D, Minami T, Iannuzzi G, Cao L, Wittenberg JB, Anzenbacher PJ, Isaacs L. *J Am Chem Soc.* 2011; 133:17966–17976. [PubMed: 21970313]
25. Huang WH, Liu S, Zavalij PY, Isaacs L. *J Am Chem Soc.* 2006; 128:14744–14745. [PubMed: 17105250] Huang WH, Zavalij PY, Isaacs L. *Angew Chem, Int Ed.* 2007; 46:7425–7427. Hettiarachchi G, Nguyen D, Wu J, Lucas D, Ma D, Isaacs L, Briken V. *PLoS One.* 2010; 5:e10514. [PubMed: 20463906] Ma D, Zavalij PY, Isaacs L. *J Org Chem.* 2010; 75:4786–4795. [PubMed: 20540586]
26. Cao L, Isaacs L. *Org Lett.* 2012; 14:3072–3075. [PubMed: 22650758]
27. Wu F, Wu LH, Zhang YQ, Xue SF, Tao Z, Day AI. *J Org Chem.* 2012; 77:606–611. [PubMed: 22121978]
28. Day AI, Arnold AP, Blanch RJ. *Molecules.* 2003; 8:74–84. Lagona J, Fettinger JC, Isaacs L. *Org Lett.* 2003; 5:3745–3747. [PubMed: 14507220] Wittenberg JB, Costales MG, Zavalij PY, Isaacs L. *Chem Commun.* 2011; 47:9420–9422.
29. Zhao Y, Xue S, Zhu Q, Tao Z, Zhang J, Wei Z, Long L, Hu M, Xiao H, Day AI. *Chin Sci Bull.* 2004; 49:1111–1116.
30. Day, AI.; Arnold, AP.; Blanch, RJ. Method for Preparing Cucurbiturils. WO 2005/026168 A1. 2005. (Unisearch Limited)
31. We choose to use 9M H₂SO₄ because this was the solvent used in the high yielding synthesis of CB[7] reported by Nau and to use KI because metal ions are known from the work of Day to influence the distribution of CB[n] obtained. Analysis of the crude reaction mixtures between **1** and **12** conducted in 9M H₂SO₄ in the absence of KI contain less **18** (CB[6]: 70%, **18**: 25%), as do reactions conducted in conc. HCl in the presence of KI (CB[6]: 70%, **18**: 30%) or the absence of KI (CB[6]: 59%, **18**: 39%) as shown in the Supporting Information. See: Marquez C, Huang F, Nau WM. *IEEE Trans Nanobiosci.* 2004; 3:39–45. Day AI, Blanch RJ, Coe A, Arnold AP. *J Inclusion Phenom Macrocyclic Chem.* 2002; 43:247–250.
32. Stella VJ, Rajewski RA. *Pharm Res.* 1997; 14:556–567. [PubMed: 9165524] De Greef TFA, Smulders MMJ, Wolffs M, Schenning APHJ, Sijbesma RP, Meijer EW. *Chem Rev.* 2009; 109:5687. [PubMed: 19769364]
33. Witt D, Lagona J, Damkaci F, Fettinger JC, Isaacs L. *Org Lett.* 2000; 2:755–758. [PubMed: 10814425] Wu A, Chakraborty A, Witt D, Lagona J, Damkaci F, Ofori MA, Chiles JK, Fettinger JC, Isaacs L. *J Org Chem.* 2002; 67:5817–5830. [PubMed: 12153286]
34. Walker S, Oun R, McInnes FJ, Wheate NJ. *Isr J Chem.* 2011; 51:616–624. Ghosh I, Nau WM. *Adv Drug Delivery Rev.* 2012; 64:764–783. Day AI, Collins JG. *Supramol Chem Mol Nanomater.* 2012; 3:983–1000.
35. Zhao Y, Buck DP, Morris DL, Pourgholami MH, Day AI, Collins JG. *Org Biomol Chem.* 2008; 6:4509–4515. [PubMed: 19039358] Koner AL, Ghosh I, Saleh Ni, Nau WM. *Can J Chem.* 2011; 89:139–147. Dong N, Xue SF, Zhu QJ, Tao Z, Zhao Y, Yang LX. *Supramol Chem.* 2008; 20:659–665.
36. Connors, KA. *Binding Constants.* John Wiley & Sons; New York: 1987.
37. Bardelang D, Udachin KA, Leek DM, Margeson JC, Chan G, Ratcliffe CI, Ripmeester JA. *Cryst Growth Des.* 2011; 11:5598–5614.
38. Kimpe ND, D'Hondt L, Stanoeva E. *Tetrahedron Lett.* 1991; 32:3879–3882.
39. Kimpe ND, Stevens C. *Tetrahedron.* 1995; 51:2387–2402.
40. Ozcubukcu S, Okzal E, Jimeno C, Pericàs M. *Org Lett.* 2009; 11:6480–6483.
41. Park KM, Kim SY, Heo J, Whang D, Sakamoto S, Yamaguchi K, Kim K. *J Am Chem Soc.* 2002; 124:2140–2147. [PubMed: 11878967] Ko YH, Kim K, Kang JK, Chun H, Lee JW, Sakamoto S, Yamaguchi K, Fettinger JC, Kim K. *J Am Chem Soc.* 2004; 126:1932–1933. [PubMed: 14971915] Da Silva JP, Jayaraj N, Jockusch S, Turro N, Ramamurthy V. *Org Lett.* 2011; 13:2410–2413. [PubMed: 21476519]

42. Cohen Y, Avram L, Frisch L. *Angew Chem Int Ed.* 2005; 44:520–554.
43. Assemblies $u,u,u,u-1_4$ and $u,u,u,d-1_4$ are chiral with enantiomers $d,d,d,d-1_4$ and $d,d,d,u-1_4$. Assemblies $u,u,d,d-1_4$ and $u,d,u,d-1_4$ are achiral due the presence of an inversion center and an S_4 axis, respectively.

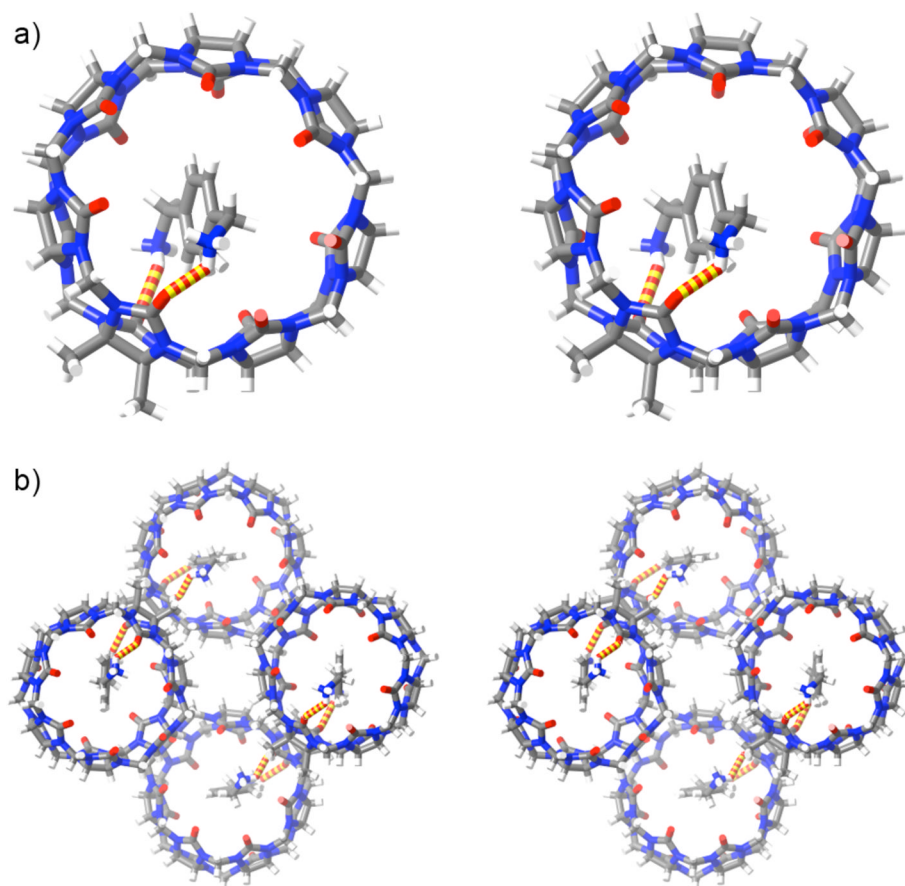


Figure 1. Cross-eyed stereoviews of: a) the x-ray crystal structure of Me₂CB[7]•3, and b) a portion of the crystal lattice showing the three dimensional packing motif. Color code: C, gray; H, white; N, blue; O, red; H-bonds, red-yellow striped.

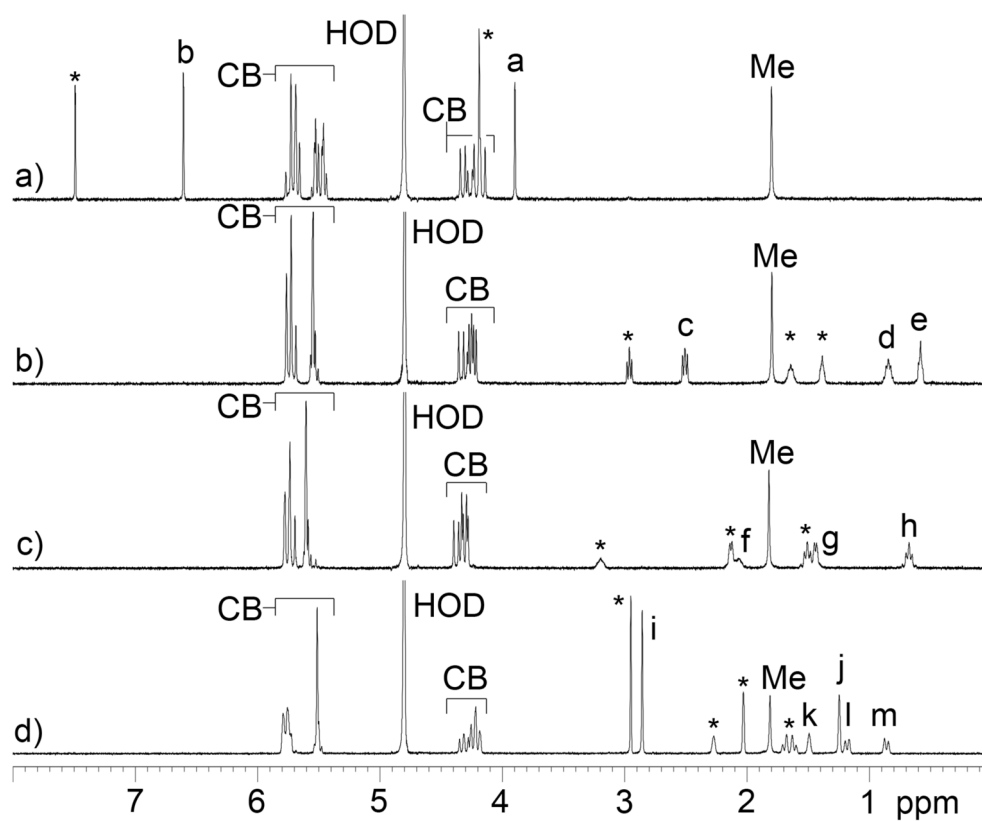


Figure 2. ^1H NMR spectra (400 MHz, D_2O , RT) recorded for mixtures of: a) $\text{Me}_2\text{CB}[7]$ and **3** (2 equiv.), b) $\text{Me}_2\text{CB}[7]$ and **4** (2 equiv.), c) $\text{Me}_2\text{CB}[7]$ and **7** (2 equiv.), d) $\text{Me}_2\text{CB}[7]$ and **10** (2 equiv.). Resonances marked with * arise from free guest.

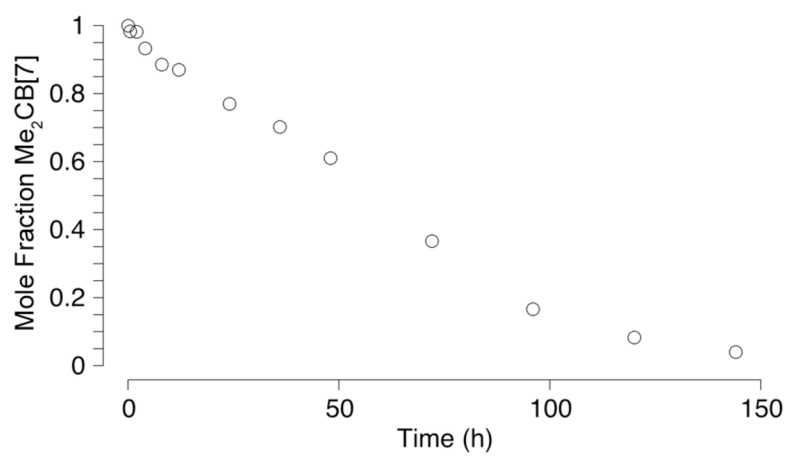


Figure 3. Plot of the mole fraction of Me₂CB[7] upon heating at 110 °C in 9M H₂SO₄ as a function of time.

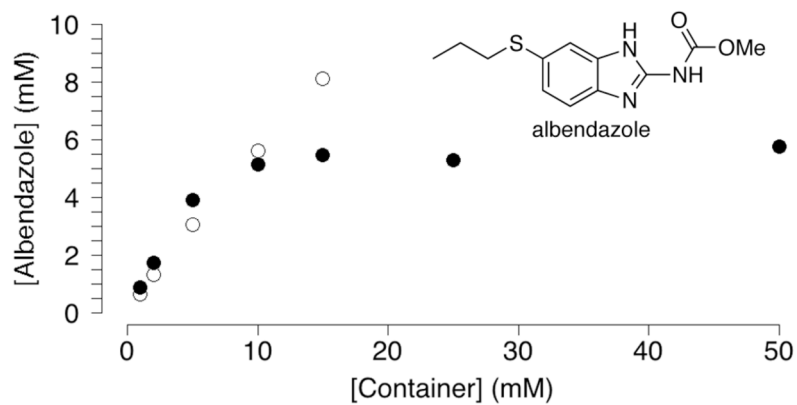


Figure 4. Phase solubility diagram constructed (D_2O , DCI , $pH\ 2.0$, room temperature) for the solubilization of albendazole in the presence of $CB[7]$ (o) or $Me_2CB[7]$ (•).

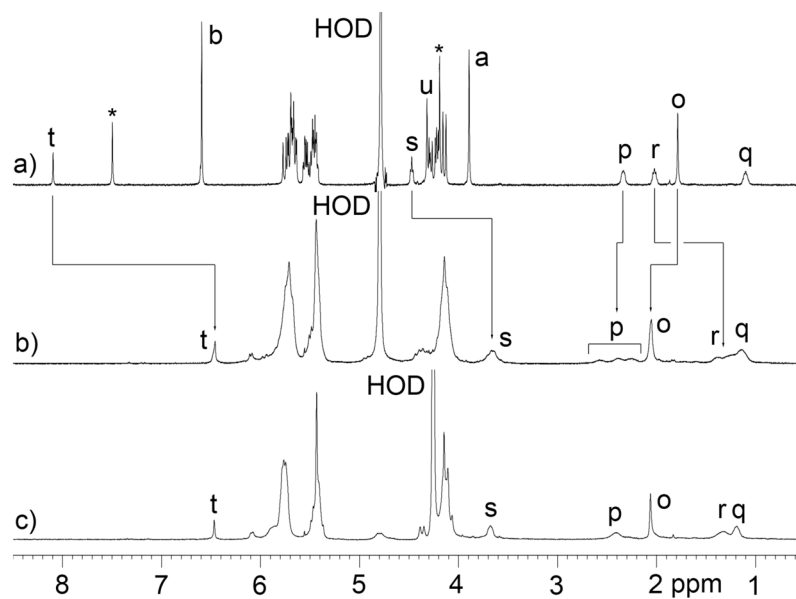


Figure 5. ^1H NMR spectra (400 MHz, D_2O) recorded for mixtures of: a) **20** and **3** (1.4 equiv.), b) **20** (3.3 mM) at 20 °C, and c) **20** (3.3 mM) at 80 °C.

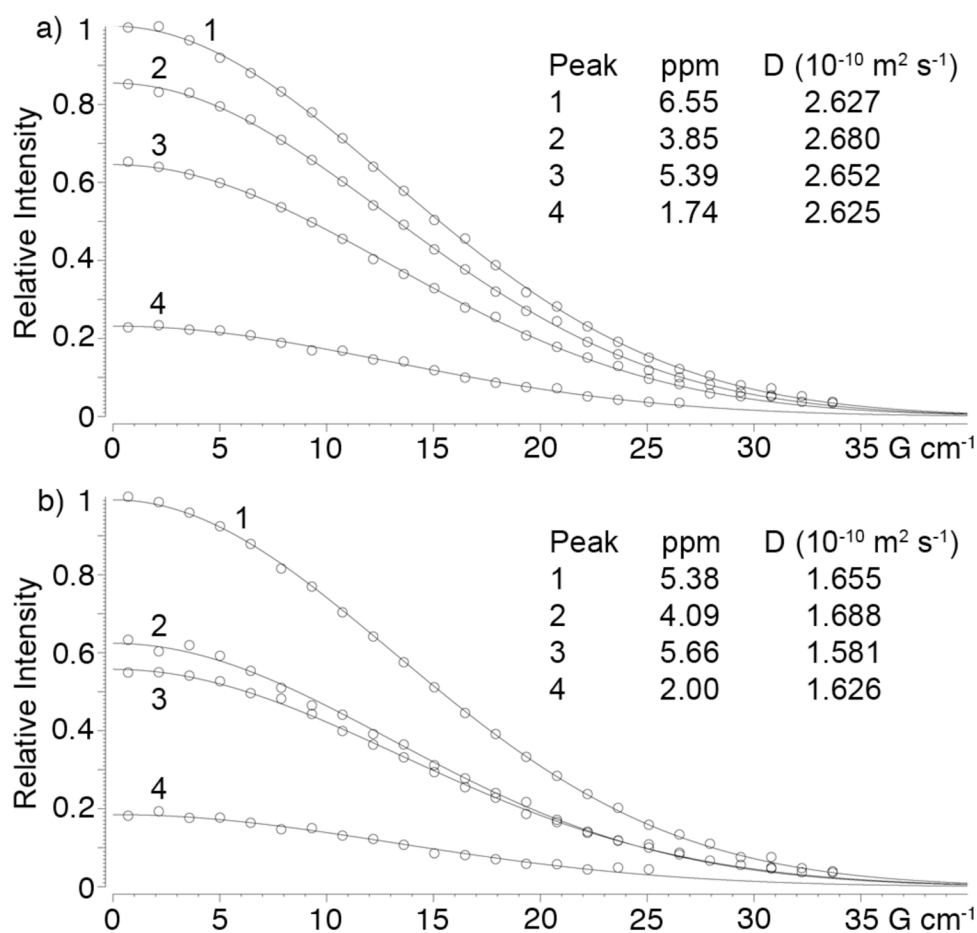


Figure 6. DOSY spectra recorded (600 MHz, D_2O , RT) for: a) $20\cdot 3$, and b) cyclic tetramer 20_4 .

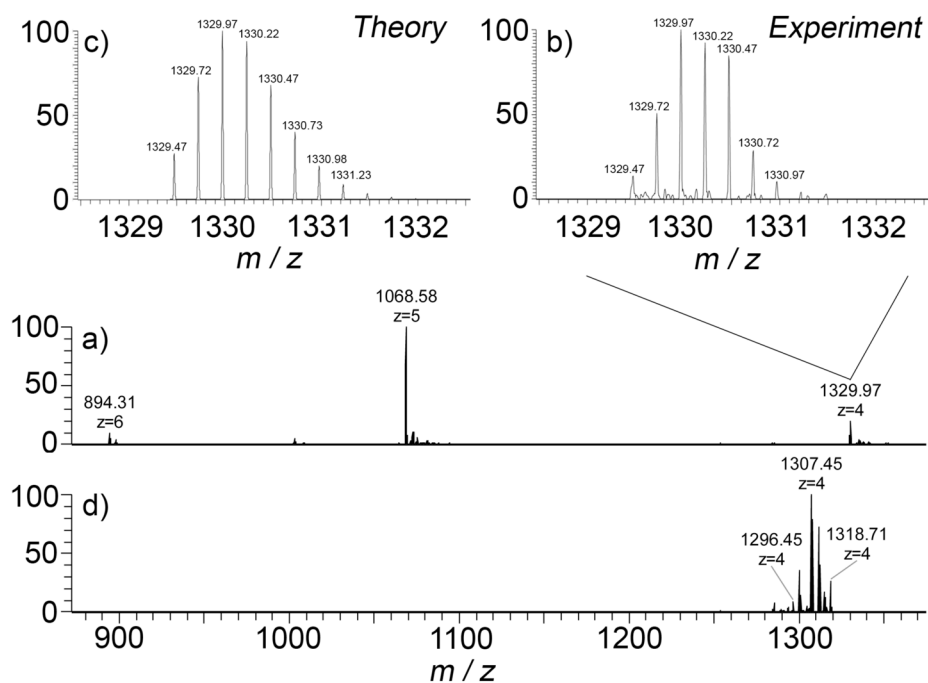
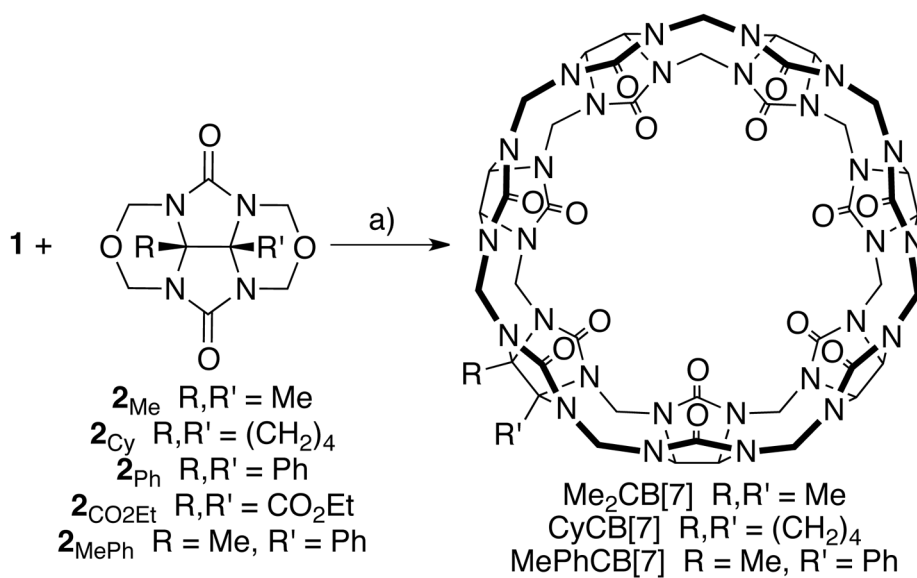
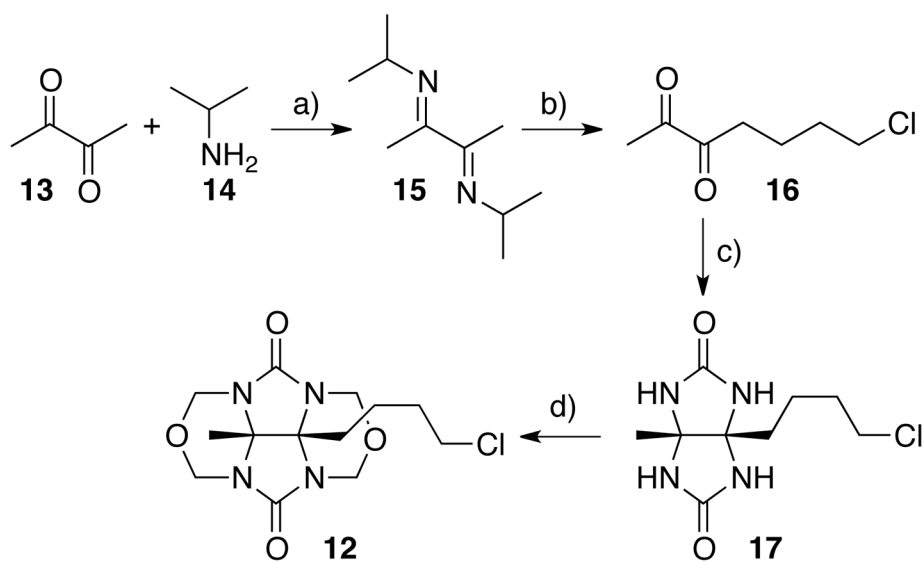


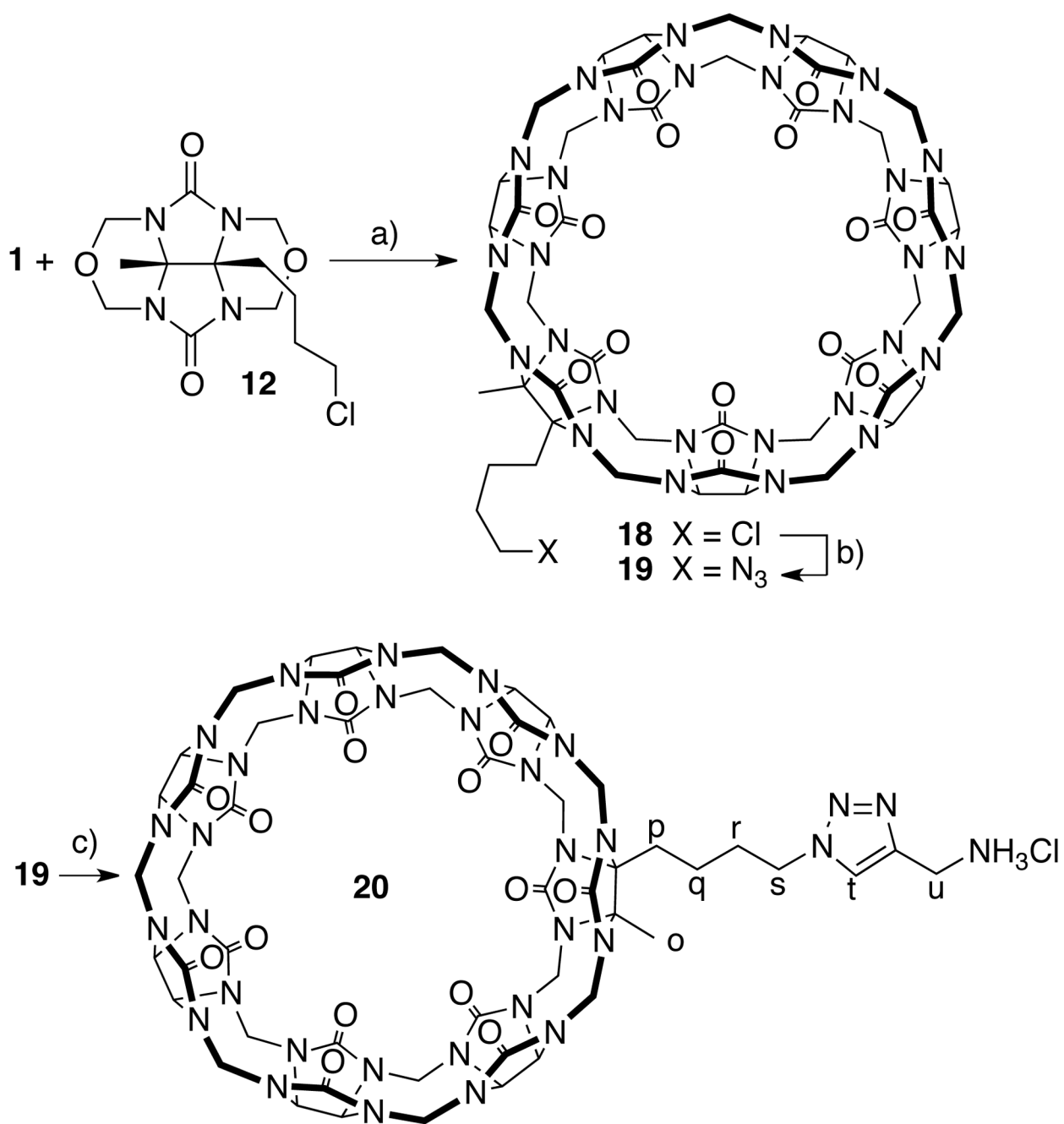
Figure 7. Electropray ionization mass spectra recorded for: a) a solution of **1**₄ (100 μ M, H₂O), b) expansion of the **1**₄⁴⁺ ion region, and c) theoretical distribution obtained for the molecular formula C₂₀₀H₂₂₈N₁₂₈O₅₆⁴⁺, and d) mass spectrum obtained upon collisional induced dissociation.

**Scheme 1.**

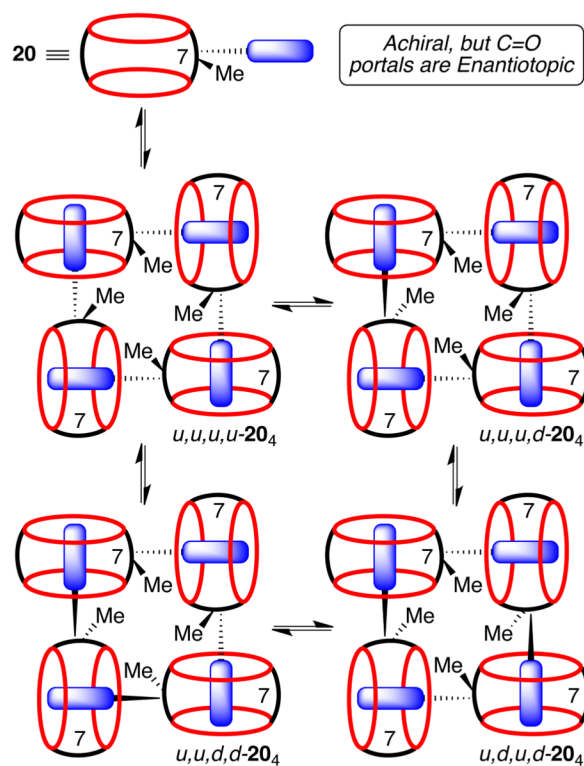
Synthesis of Me₂CB[7], CyCB[7], and MePhCB[7]. Conditions: a) 9M H₂SO₄, 110 °C, KI, 30 min.

**Scheme 2.**

Synthesis of glycoluril derivative **12**. Conditions: a) Et_2O , TiCl_4 , b) LDA, THF, $\text{Cl}(\text{CH}_2)_3\text{I}$, 69%, c) HCl, urea, 35%, d) HCl, formalin, 68%.

**Scheme 3.**

Synthesis of CB[7] derivatives **18** – **20**. Conditions: a) 9M H₂SO₄, KI, 110 °C, 16%, b) NaN₃, 80 °C, 81%, c) **21**, Pericàs' catalyst, H₂O, 50 °C, 95%.

**Scheme 4.**

Self-assembly of CB[7] derivative **20** to give the cyclic tetramer **20₄** as a mixture of diastereomers.

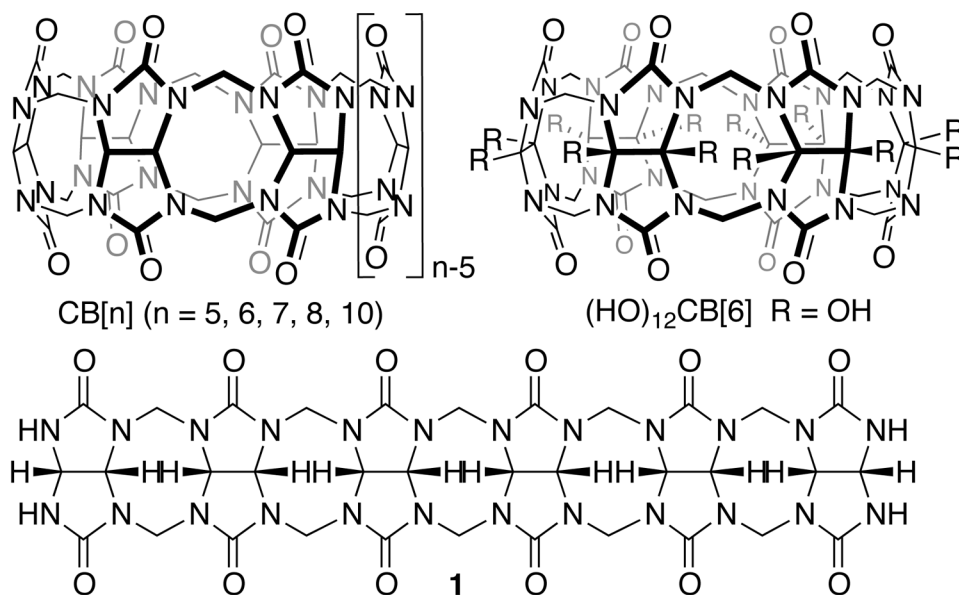


Chart 1.
Structure of $CB[n]$, $(HO)_{12}CB[6]$, and hexamer **1**.

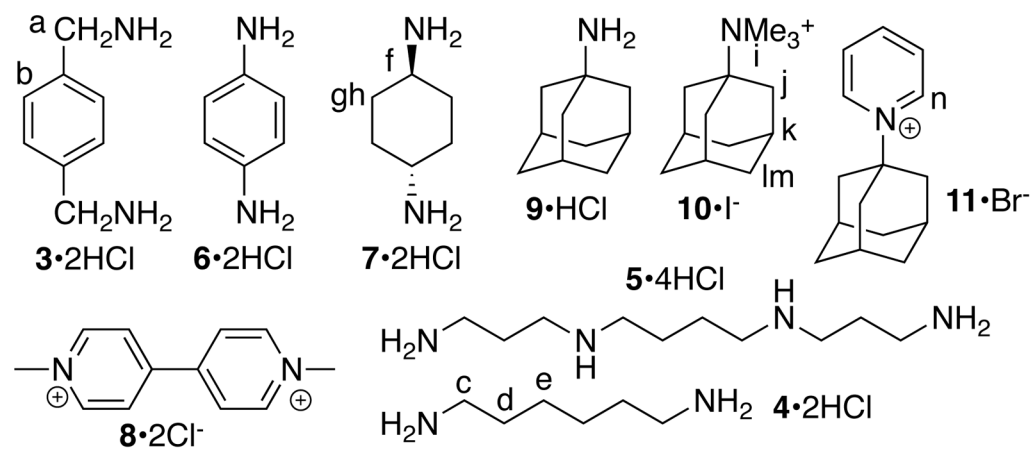


Chart 2.
Structure of guests used in this study.